Chinese Chemical Letters xxx (2015) xxx–xxx

Contents lists available at ScienceDirect

Chinese Chemical Letters

journal homepage: www.elsevier.com/locate/cclet

Original article

# Characterization and reactivity of $\gamma$-$Al_2O_3$ supported Pd–Ni bimetallic nanocatalysts for selective hydrogenation of cyclopentadiene

Yi-Si Feng [a,b,c], Jian Hao [a], Wei-Wei Liu [a], Yun-Jin Yao [a], Yue Cheng [a], Hua-Jian Xu [a,*]

[a] School of Chemistry and Chemical Engineering, School of Medical Engineering, Hefei University of Technology, Hefei 230009, China
[b] Anhui Key Laboratory of Controllable Chemical Reaction & Material Chemical Engineering, Hefei 230009, China
[c] Anhui Provincial Laboratory of Heterocyclic Chemistry, Maanshan 243110, China

ARTICLE INFO

*Article history:*
Received 26 December 2014
Received in revised form 20 January 2015
Accepted 9 February 2015
Available online xxx

*Keywords:*
Impregnation method
Hydrogenation
Cyclopentadiene
Cyclopentene
Pd–Ni/$Al_2O_3$

ABSTRACT

Several $\gamma$-$Al_2O_3$ supported Pd–Ni bimetallic nanocatalysts (Pd–Ni ($x$:$y$)/$Al_2O_3$; where $x$ and $y$ represent the mass ratio of Pd and Ni, respectively) were prepared by the impregnation method and used for selective hydrogenation of cyclopentadiene to cyclopentene. The Pd–Ni/$Al_2O_3$ samples were confirmed to generate Pd–Ni bimetallic nanoparticles by X-ray diffraction (XRD), X-ray photoelectron spectroscopy (XPS) and transmission electron microscopy (TEM). The catalytic activity was assessed in view of the effects of different mass ratios of Pd and Ni, temperature, pressure, *etc.* Among all the samples, the Pd–Ni (1:1)/$Al_2O_3$ (PN-1:1) catalyst showed extremely high catalytic ability. The conversion of cyclopentadiene and selectivity for cyclopentene can be simultaneously more than 90%.


## 1. Introduction

Cyclopentene is of significant value as a raw and process material for the production of special rubbers, cyclopentanone, cyclopentanol, bromocyclopentane and chlorocyclopentane in chemical manufacturing applications. In general, cyclopentadiene is reduced to manufacture cyclopentene, which is a green and effective method. The role of catalyst is a crucial factor in the selective hydrogenation reaction [1–3], which leads to research of heterogeneous catalysts as the core of experimentation. The earlier literature reported Raney nickel as a catalyst for the selective hydrogenation of cyclopentadiene to cyclopentene [4]. Nevertheless, cyclopentene can be easily reduced to cyclopentane by Raney nickel, but leads to results of poor selectivity of the catalyst, low yield, and many byproducts. Some researchers applied noble metal particles, such as Pd, Pt and Ru, which also had been demonstrated as effective catalysts [5,6]. However, the main drawbacks of the precious metal catalysts are low selectivity and cost (extensive use of noble metals). Other sources reported that an organic membrane reactor could be effectively applied in the selective hydrogenation of cyclopentadiene in a gas-phase reaction [1,7–9]. Nevertheless, the above method also has many defects, such as difficult cleaning, high cost, short service life, *etc.* Therefore, it is necessary to explore a highly efficient and reliable catalyst to improve production process.

Recently, supported nanometal catalysts, especially bimetal nanocatalysts, have obtained much attention due to their conspicuous catalytic ability, high stability and outstanding recyclability. Compared with monometallic catalysts, bimetallic catalysts display excellent catalytic ability and selectivity because of the flexible proportional change of the two components. Meanwhile, nanometal catalysts have been used in hydrogenation of arenes and olefins [10–13]. The Marck group employed Pd–Ni bimetallic catalysts in the hydrogenation of *p*-chloronitrobenzene, which showed excellent catalytic ability and selectivity [12]. Other researchers applied Pd–Ni bimetallic samples in the hydrodechlorination of chlorobenzene, which also displayed infrequent chlorine tolerance and constant catalytic activity during the reaction process [13]. To the best of our knowledge, $\gamma$-$Al_2O_3$ supported Pd–Ni nanocatalysts (Pd–Ni/$Al_2O_3$) have not been used in selective hydrogenation of cyclopentadiene.

Herein, we synthesized Pd–Ni/$Al_2O_3$ catalysts, used as a heterogeneous catalyst for the hydrogenation of cyclopentadiene. Different characterization techniques, such as X-ray diffraction (XRD), X-ray photoelectron spectroscopy (XPS) and transmission electron microscopy (TEM), were employed to determine the structural features of Pd–Ni/$Al_2O_3$. Additionally, the impacts of various factors were studied to explore the best reaction conditions.

* Corresponding author.
*E-mail address:* hjxu@hfut.edu.cn (H.-J. Xu).

http://dx.doi.org/10.1016/j.cclet.2015.03.006


Please cite this article in press as: Y.-S. Feng, et al., Characterization and reactivity of $\gamma$-$Al_2O_3$ supported Pd–Ni bimetallic nanocatalysts for selective hydrogenation of cyclopentadiene, Chin. Chem. Lett. (2015), http://dx.doi.org/10.1016/j.cclet.2015.03.006

The purpose of this paper is to find an efficient and recyclable catalyst of selective hydrogenation.

## 2. Experimental

### 2.1. Preparation of Pd–Ni/$Al_2O_3$ catalysts

The Pd–Ni/$Al_2O_3$ catalysts were prepared by the impregnation method [12,15–17]. In a typical Pd–Ni (1:1)/$Al_2O_3$ (PN-1:1) catalyst synthesis process, $PdCl_2$ (12.7 mg) and $Ni(NO_3)_2{\cdot}6H_2O$ (37.5 mg) were dissolved in 10 mL acetic acid solution (0.0225 mol/L) with constant agitation (500 rpm) at room temperature. Then, to this clear solution was slowly added $\gamma$-$Al_2O_3$ (1.5 g) and uniformly stirred with 300 rpm for 5 h. After impregnation, the solution was heated to 100 °C to remove the redundant $H_2O$ to yield a sticky substance, which was dried in a vacuum oven at 80 °C for 12 h. Afterwards, the obtained catalyst forerunners were ground to powder and calcined in nitrogen (0.3 L/min) from room temperature to 500 °C at a rate of 40 °C/min, then kept at 500 °C for 4 h. Subsequently, the sample precursors were reduced by hydrogen (0.15 L/min) in nitrogen at 500 °C for 2 h and, finally, the PN-1:1 catalyst was obtained. In order to research the effect of the loading of metals, catalysts of different Pd/Ni mass ratios were synthesized to apply in the hydrogenation reaction.

### 2.2. Characterization

The XRD of different samples were recorded on a Rigaku D/MAX 2500 V diffractometer with Cu Kα radiation and scanned at a rate of 10°/min over the range 20–80°. The XPS analysis was confirmed on the Thermo Fisher Scientific ESCALAB 250 under excessive vacuum condition using a monochromatic Al $K_\alpha$ gun with photonic energy of 1486.6 eV as X-ray source. The binding energies (B.E.) acquired in the XPS analysis were compensated by using the C 1 s (284.6 eV) signal for any charging effects. The TEM images of catalysts were obtained on a JEOL JEM-2100F electron microscope equipped with EDS performed at an accelerating voltage of 120 kV. Samples were prepared by ultrasonic dispersion in ethanol and deposited on a copper grid for analysis.

### 2.3. Catalytic reaction

In a typical procedure, three different materials were mixed together, including cyclopentadiene (0.24 mol) as a raw material, cyclohexane (0.93 mol) as solvent and PN-1:1 (0.32 g, 2.0 wt% of cycleopentadiene) as catalyst. The mixtures were stirred (400 rpm) in an autoclave under 1.0 MPa hydrogen pressure at 35 °C for 1.5 h. The above conditions were the optimal. In addition, the impact of various factors and reusability (Fig. S1 in Supporting information) of PN-1:1 was also investigated.

## 3. Results and discussion

### 3.1. Characterization of catalysts

#### 3.1.1. X-ray diffraction

The XRD patterns of Ni/$Al_2O_3$ and diverse Pd–Ni/$Al_2O_3$ catalysts are exhibited in Fig. 1. The results show a low intensity level for all characteristic diffraction planes, except for the planes associated with the $\gamma$-$Al_2O_3$ support [18]. For $\gamma$-$Al_2O_3$, four apparent signals at $2\theta = 32.8°, 37.4°, 45.8°, 67.2°$ are detected which correspond to the (0 2 2), (0 2 5), (2 2 0) and (0 4 2) facets (JCPDS 04-0877), respectively. Nevertheless, Ni peaks have not been found in all samples, perhaps due to the reduced loading Ni and the generation of nickel ions. According to the literature [13,19], the XRD patterns of Pd–Ni bimetallic catalysts also do not display the precise Ni phase in accordance with our research results. Fig. 1E and F exhibit visible Pd peaks at $2\theta = 40.1°$ corresponding to the characteristic phases of the (1 1 1) Pd planes (JCPDS 46-1043) [12]. The Pd peaks are gradually strengthened with increasing Pd content. Meanwhile, the signals at $2\theta = 45.8°$ and 67.2° (Fig. 1E and F) are different from other corresponding signals (Fig. 1B–D), which illustrates the phases of (2 0 0) and (2 2 0) Pd planes at $2\theta = 46.7°$ and 68.1° are conceivably hidden by the $\gamma$-$Al_2O_3$ signals. In Fig. 1B–D, the Pd phase at $2\theta = 40.1°$ is inconspicuous, which may be due to the trace amounts of Pd used to prepare the catalysts. In addition, the calculated results indicate that the size of the Pd crystalline grain (Fig. 1E and F) is around 2.23 nm by the Scherrer formula. In conclusion, we need to further confirm the hypothetic Pd–Ni bimetallic nanoparticles in catalysts by XPS and TEM analysis.

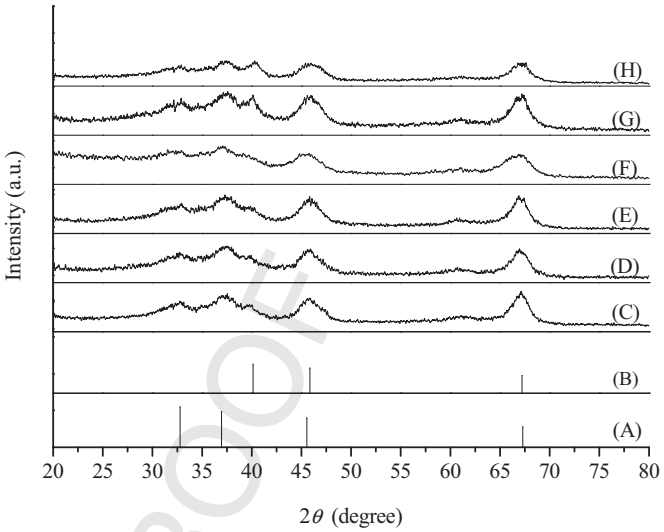


**Fig. 1.** XRD patterns of (A) $\gamma$-$Al_2O_3$ (JCPDS 04-0877), (B) Pd (JCPDS 46-1043), (C) Ni, (D) PN-1:3, (E) PN-1:2, (F) PN-1:1, (G) PN-2:1, (H) PN-3:1.

#### 3.1.2. X-ray photoelectron spectroscopy

XPS analysis is used to determine the electronic properties of metal components. The XPS spectra are exhibited in Fig. 2. The B.E. of Pd $3d_{5/2}$ and Ni $2p_{3/2}$ of the diverse catalysts are shown in Table 1. The Pd $3d_{5/2}$ B.E. of Pd/$Al_2O_3$ is 336.1 eV (Fig. 2A), which is inconsistent with the determination of B.E. of zero valent palladium ($335.2 \pm 0.2$ eV) as a result of the existence of $Pd^{n+}$ species [13]. According to the literature, a strong metal–support interaction may lead to the generation of $Pd^{n+}$ species. In Fig. 2A–C, 335.4, 335.3, 335.4, 335.2 and 335.4 eV are attributed to Pd $3d_{5/2}$ B.E. of various Pd–Ni/$Al_2O_3$ catalysts. The B.E. of Pd $3d_{5/2}$ is $335.3 \pm 0.1$ and 336.1 eV in all the catalysts, which correspond to Pd and PdO, respectively [12,19]. Therefore, the primary state of Pd in the Pd/$Al_2O_3$ catalyst is PdO, while zero valent palladium is the main valence state of Pd in diverse Pd–Ni/$Al_2O_3$ samples. The change of Pd $3d_{5/2}$ B.E. between different Pd–Ni/$Al_2O_3$ catalysts and Pd/$Al_2O_3$ catalyst is due to the combining of the Ni component with the Pd constituent to form Pd–Ni bimetallic nanoparticles [12,20].

Similar to the results of Pd $3d_{5/2}$ B.E, data in Table 1 demonstrates that the Ni $2p_{3/2}$ B.E. of the various Pd–Ni/$Al_2O_3$ catalysts are different from the Ni/$Al_2O_3$ catalyst, which confirms illustrates that Pd and Ni have an intimate contact. The Ni 2p B.E. regions of diverse catalysts are shown in Fig. 2D–F. It is well known that the B.E. of Ni $2p_{3/2}$ at 852.0 and 856.0 eV are assigned to metallic Ni and NiO, respectively [13,21]. In the present case, the B.E. of Ni $2p_{3/2}$ of different catalysts are observed at $(855.3 \pm 0.2)$ eV and $(856.0 \pm 0.1)$ eV, which approximates the B.E. of NiO phases [19]. Thus, all the catalysts have NiO phases. The discrepancy of Ni $2p_{3/2}$ B.E. of all the catalysts is due to the transfer of



Please cite this article in press as: Y.-S. Feng, et al., Characterization and reactivity of $\gamma$-$Al_2O_3$ supported Pd–Ni bimetallic nanocatalysts for selective hydrogenation of cyclopentadiene, Chin. Chem. Lett. (2015), http://dx.doi.org/10.1016/j.cclet.2015.03.006

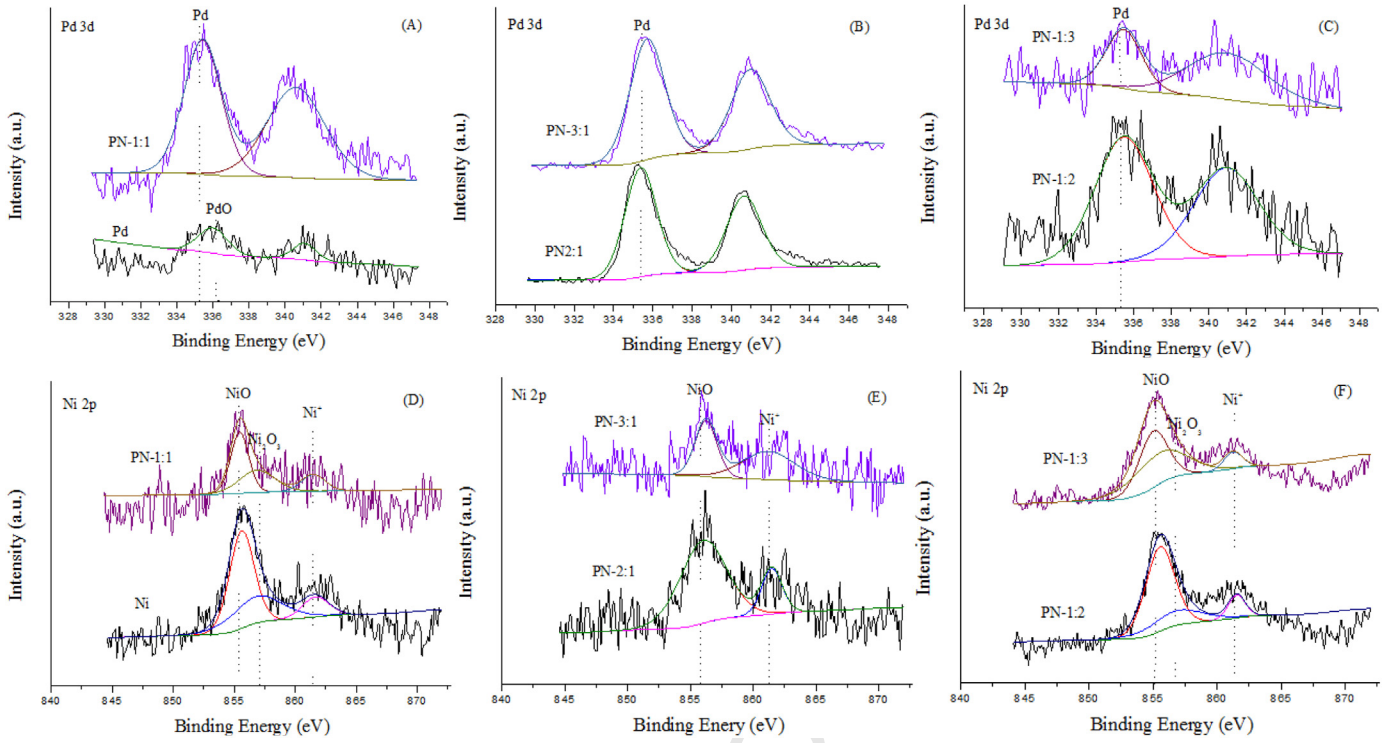


**Fig. 2.** XPS spectra of all catalysts. (A) Pd 3d peaks of Pd and PN1:1, (B) Pd 3d peaks of PN-2:1 and PN-3:1, (C) Pd 3d peaks of PN-1:2 and PN-1:3, (D) Ni 2p peaks of Ni and PN-1:1, (E) Ni 2p peaks of PN-2:1 and PN-3:1, (F) Ni 2p peaks of PN-1:2 and PN-1:3.

electron density between Pd and Ni caused by the diverse amounts of Pd and Ni [13,22]. In addition, the peak at 857 eV (Fig. 2D and F) is $Ni_2O_3$ [23] also inhibited with the increase of the amounts of Pd (Fig. 2E). The B.E. of satellite peaks of $Ni^{2+}$ are 861.3 eV [19]. In conclusion, Pd–Ni bimetallic nanoparticles were detected in the Pd–Ni/$Al_2O_3$ catalysts.

Furthermore, the surface atom percentages of Pd and Ni are shown in Table 1, which illustrates that the increase of Pd (or Ni) leads to the invisibility of Ni (or Pd) on the surface of catalysts. According to the XPS spectra, the metals are introduced into the core of $\gamma$-$Al_2O_3$, which leads to its invisibility. Meanwhile, the quantities of invisible metals are tiny, which are covered by the visible metal. The above results illustrate that an appropriate ratio (1:1) of Pd and Ni leads to the simultaneous distribution of the two metals on the surface of the catalysts [13,20].

### 3.1.3. Transmission electron microscopy

The microstructure of PN-1:1 catalyst is observed by TEM and Fig. 3A and B show that similar spherical particles are well-dispersed on the support. The size distribution histogram (Fig. 3C) clearly shows the diameters of the metal particles range from 4 nm to 13 nm (average size 7.91 nm). In the EDS result (Fig. 3D), the presence of O, Al, Ni and Pd atoms with color characterization in PN-1:1 catalyst noted, which shows that nickel and palladium have been introduced into the $\gamma$-$Al_2O_3$ support. Electron mapping image analysis (Fig. 3E and F) shows the distribution of oxygen (O), aluminum (Al), nickel (Ni) and palladium (Pd) atoms with red, green, blue and pink colors, respectively, which further confirms the homogeneous distribution of Pd–Ni bimetallic nanoparticles on the surface of the $\gamma$-$Al_2O_3$ support.

**Table 1**
XPS data of catalysts.

| Catalyst | Binding energy (eV) | | Pd:Ni (atom %)[a] |
|---|---|---|---|
| | Pd $3d_{5/2}$ | Ni $2p_{3/2}$ | |
| Pd | 336.1 | – | – |
| PN-3:1 | 335.4 | 856.1 | 0.67:0 |
| PN-2:1 | 335.2 | 856.0 | 0.41:0 |
| PN-1:1 | 335.4 | 855.3 | 0.14:0.25 |
| PN-1:2 | 335.3 | 855.2 | 0:0.4 |
| PN-1:3 | 335.4 | 855.2 | 0:0.63 |
| Ni | – | 855.5 | – |

[a] The proportion of atomic percentage of Pd and Ni.

### 3.2. Activity measurements

The catalytic activity of the various samples was measured for selective hydrogenation of cyclopentadiene under different conditions (Table 2). The results showed that all catalysts had a catalytic ability of the hydrogenation reaction except for Ni/$Al_2O_3$, which illustrated palladium is the essential component of catalysts. Meanwhile, PN-1:1 catalyst exhibited the best catalytic ability during the process of reaction. Compared with PN-1:1, the catalytic activity of PN-1:2 and PN-1:3 was passivated, which was due to the decrease of Pd species on support surface (according to XPS results) with increasing amounts of nickel in the catalysts. Similarly, the hydrogenation reaction was also retarded with increasing the amounts of palladium. It was apparent that hydrogenation of cyclopentadiene catalyzed by Pd–Ni/$Al_2O_3$ need the appropriate proportion of Pd and Ni. The inferior catalytic activity of Pd/$Al_2O_3$ samples was perhaps due to plentiful PdO (according to XPS measurement) dispersed on the surface of catalyst. In addition, the catalytic activity of Pd/$Al_2O_3$ + Ni/$Al_2O_3$ and Pd/$Al_2O_3$ was similar, which illustrated that the Pd–Ni bimetal was the crucial factor of the hydrogenation reaction. Simultaneously, the XPS and TEM measurements for PN-1:1 catalyst demonstrated the homogeneous distribution of Pd–Ni bimetallic nanoparticles on the sample surface. We suggest that the above reasons led to PN-1:1 and showed the best catalytic performance. The temperature, pressure, speed (rate) and amounts of catalyst are all factors in the selective hydrogenation reaction. With the



Please cite this article in press as: Y.-S. Feng, et al., Characterization and reactivity of $\gamma$-$Al_2O_3$ supported Pd–Ni bimetallic nanocatalysts for selective hydrogenation of cyclopentadiene, Chin. Chem. Lett. (2015), http://dx.doi.org/10.1016/j.cclet.2015.03.006

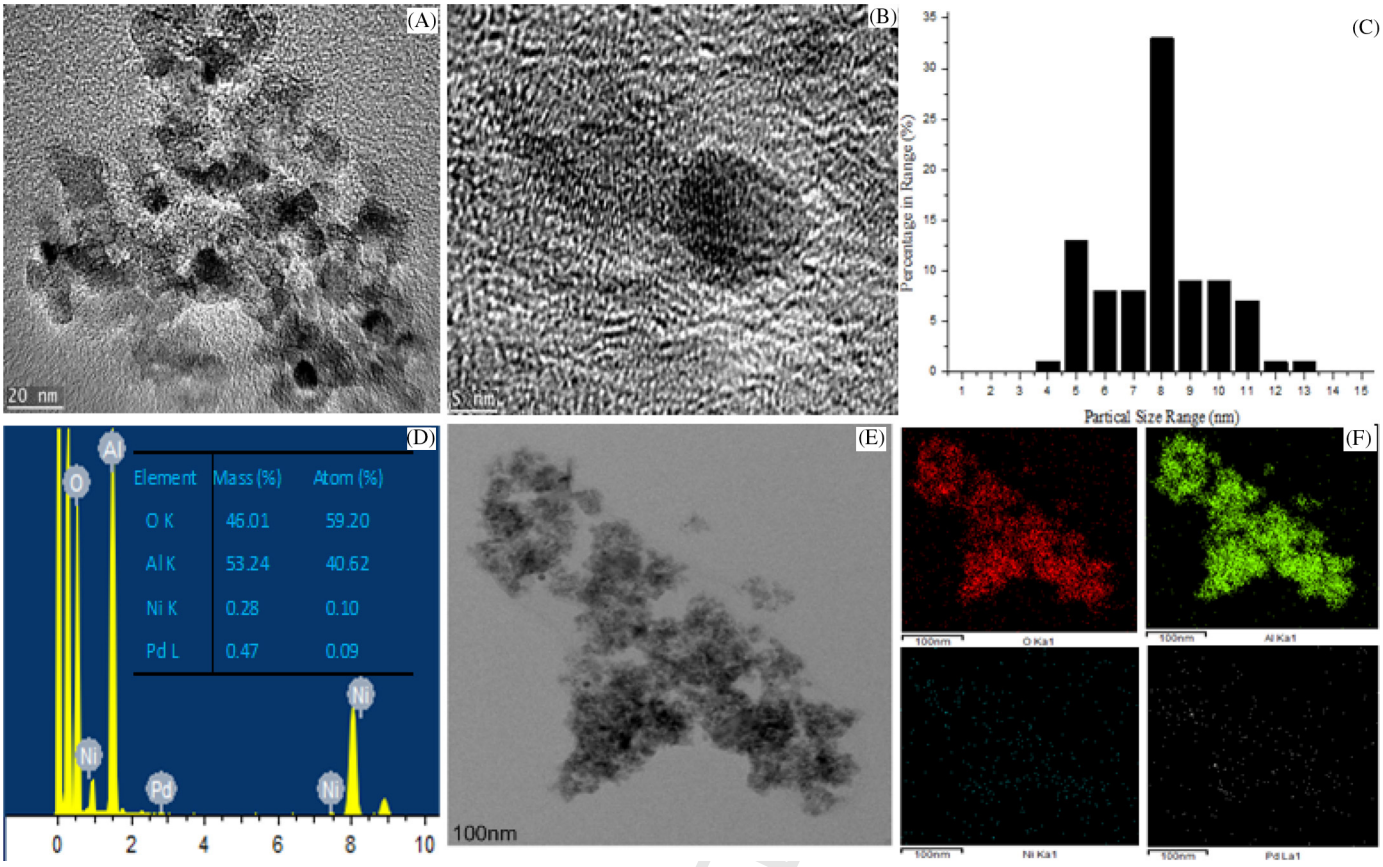


**Fig. 3.** (A) and (B) TEM images of PN-1:1, (C) metal particle size distribution, (D) EDS image, (E) and (F) electron mapping images.

**Table 2**
The hydrogenation results of cyclopentadiene.

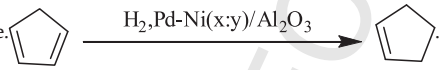


| Entry | Catalyst | Solvent | Temp. (°C) | Time (h) | Conv. (%) | Sele. (%) | Reaction rate (mol/(L min))[a] |
|---|---|---|---|---|---|---|---|
| 1 | Pd | Cyclohexane | 35 | 4 | 88 | >99 | $0.733 \times 10^{-2}$ |
| 2 | PN-3:1 | Cyclohexane | 35 | 4 | 92 | >99 | $0.767 \times 10^{-2}$ |
| 3 | PN-2:1 | Cyclohexane | 35 | 4 | 91 | >99 | $0.758 \times 10^{-2}$ |
| 4 | PN-1:1 | Cyclohexane | 35 | 1.5 | 95 | >99 | $2.11 \times 10^{-2}$ |
| 5[b] | PN-1:1 | Ethanol | 35 | 2 | 93 | >99 | $1.55 \times 10^{-2}$ |
| 6[c] | PN-1:1 | 1,2-Dichloroethane | 35 | 4 | – | – | 0 |
| 7 | PN-1:1 | Cyclohexane | 45 | 3.5 | 91 | >99 | $0.867 \times 10^{-2}$ |
| 8 | PN-1:1 | Cyclohexane | 55 | 4 | 90 | >99 | $0.750 \times 10^{-2}$ |
| 9 | PN-1:1 | Cyclohexane | 25 | 8 | 83 | >99 | $0.346 \times 10^{-2}$ |
| 10[d] | PN-1:1 | Cyclohexane | 35 | 4 | 25 | >99 | $0.208 \times 10^{-2}$ |
| 11[e] | PN-1:1 | Cyclohexane | 35 | 5 | 92 | >99 | $0.613 \times 10^{-2}$ |
| 12[f] | PN-1:1 | Cyclohexane | 35 | 4 | 90 | >99 | $0.750 \times 10^{-2}$ |
| 13[g] | PN-1:1 | Cyclohexane | 35 | 8 | 59 | >99 | $0.246 \times 10^{-2}$ |
| 14 | PN-1:2 | Cyclohexane | 35 | 8 | 55 | >99 | $0.229 \times 10^{-2}$ |
| 15 | PN-1:3 | Cyclohexane | 35 | 8 | 40 | >99 | $0.167 \times 10^{-2}$ |
| 16[h] | Pd + Ni | Cyclohexane | 35 | 4 | 85 | >99 | $0.708 \times 10^{-2}$ |
| 17 | Ni | Cyclohexane | 35 | 8 | – | – | 0 |
| 18 | Ni | Cyclohexane | 55 | 8 | – | – | 0 |
| 19[i] | PN-1:1 | Cyclohexane | 35 | 5 | 75 | >99 | $0.500 \times 10^{-2}$ |
| 20[j] | PN-1:1 | Cyclohexane | 35 | 4 | 85 | >99 | $0.708 \times 10^{-2}$ |

Reaction conditions: 0.24 mol cyclopentadiene, 0.93 mol cyclohexane, 450 rpm, catalyst (0.32 g, 2.0 wt% of cyclopentadiene) and 1.0 MPa hydrogen pressure.

[a] Reaction rate = $\Delta c/\Delta t$, $\Delta c = c_{\text{cyclopentadiene}}^{(\text{before reaction})} - c_{\text{cyclopentadiene}}^{(\text{after reaction})}$, $\Delta t$ = reaction time (from this table).

[b] 0.93 mol ethanol, other conditions are the same.

[c] 0.93 mol 1,2-dichloroethane, other conditions are the same.

[d] 0.5 MPa hydrogen pressure.

[e] 1.5 MPa hydrogen pressure.

[f] 0.24 g PN-1:1 catalyst (1.5 wt% of cyclopentadiene).

[g] 0. 40 g PN-1:1 catalyst (2.5 wt% of cyclopentadiene).

[h] Mixture of 0.16 g $Pd/Al_2O_3$ and 0.16 g $Ni/Al_2O_3$.

[i] 250 rpm.

[j] 650 rpm.



Please cite this article in press as: Y.-S. Feng, et al., Characterization and reactivity of $\gamma$-$Al_2O_3$ supported Pd–Ni bimetallic nanocatalysts for selective hydrogenation of cyclopentadiene, Chin. Chem. Lett. (2015), http://dx.doi.org/10.1016/j.cclet.2015.03.006

change of these factors, catalytic results were also transformed. When the values of those factors were neither too high nor too low, an optimal condition was produced. Subsequently, the impact of solvents (1,2-dichloroethane, ethanol, cyclohexane) was also studied for the reaction and we ascertained cyclohexane as the solvent, 35 °C, 1 Mpa hydrogen pressure, 450 rpm and PN-1:1 catalyst (2.0 wt% of cyclopentadiene) were the optimal reaction conditions.

## 4. Conclusion

In conclusion, we developed $\gamma$-$Al_2O_3$ supported mono- (Ni or Pd), mixed- (Pd and Ni) and bi-metallic (Pd–Ni) catalysts for the hydrogenation of cyclopentadiene. The best outcome confirmed the conversion of cyclopentadiene and selectivity for cyclopentene could be simultaneously more than 90% by employing the PN-1:1 catalyst under mild reaction conditions. The excellent activity of the PN-1:1 catalyst was attributed to the homogeneous distribution of Pd–Ni bimetallic nanoparticles on the surface of the support, and furthermore, the reusability (Fig. S1) of PN-1:1 is show to be excellent. Our protocol provides a potential method of producing cyclopentene in commercial production.

## Q2 Uncited reference

[14].

## Acknowledgments

Q3 We are grateful to the financial assistance from the National Natural Science Foundation of China (Nos. 21272050, 21371044, 21472033) and the Program for New Century Excellent Talents in University of the Chinese Ministry of Education (No. NCET-11-0627).

## Appendix A. Supplementary data

Supplementary data associated with this article can be found, in the online version, at http://dx.doi.org/10.1016/j.cclet.2015.03.006.

## References

[1] C.Q. Liu, Y. Xu, S.J. Liao, D.R. Yu, Selective hydrogenation of cyclopentadiene in mono- and bimetallic catalytic hollow-fiber reactors, J. Mol. Catal. A: Chem. 157 (2000) 253–259.
[2] H.R. Gao, S.J. Liao, Y. Xu, et al., Selective hydrogenation of cyclopentadiene in a catalytic cellulose acetate hollow-fiber reactor, Catal. Lett. 27 (1994) 297–303.
[3] H.R. Gao, Y. Xu, S.J. Liao, et al., Catalytic polymeric hollow-fiber reactors for the selective hydrogenation of conjugated dines, J. Membr. Sci. 106 (1995) 213–219.
[4] A.F. Plate, V.I. Stanko, Preparation of cyclopentene from cyclopentadiene, Bull. Acad. Sci. USSR Div. Chem. Sci. 5 (1956) 1173–1174.
[5] V.M. Gryaznov, M.M. Ermilova, L.D. Gogua, N.V. Orekhova, L.S. Morozova, Hydrogenation of cyclopentadiene in the presence of isoprene and 1,3-pentadiene on a Pd–Ru membrane catalyst, Bull. Acad. Sci. USSR Div. Chem. Sci. 30 (1981) 672–675.
[6] L.K. Freidlin, B.D. Polkovnikov, Hydrogenation of cyclopentadiene in binary mixtures with unsaturated hydrocarbons on palladium and platinum blacks, Bull. Acad. Sci. USSR Div. Chem. Sci. 6 (1957) 555–559.
[7] N. Itoh, W.C. Xu, A.M. Sathet, Capability of permeate hydrogen through palladium-based membranes for acetylene hydrogenation, Ind. Eng. Chem. Res. 32 (1993) 2614–2619.
[8] K. Eiichi, Palladium/ceramic membranes for selective hydrogen permeation and their application to membrane reaction, Catal. Today 25 (1995) 333–337.
[9] C.Q. Liu, Y. Xu, S.J. Liao, D.Y. Yu, Mono- and bimetallic catalytic hollow-fiber reactors for the selective hydrogenation of butadiene in 1-butene, Appl. Catal. A: Gen. 172 (1998) 23–29.
[10] W.J. Wang, M.H. Qiao, H.X. Li, J.F. Deng, Amorphous NiP/$SiO_2$ aerogel: its preparation, its high thermal stability and its activity during the selective hydrogenation of cyclopentadiene to cyclopentene, Appl. Catal. A: Gen. 166 (1998) L243–L247.
[11] S. Yoshida, H. Yamashita, T. Funabiki, T. Yonezawa, Catalysis by amorphous metal alloys. Part 1—hydrogenation of olefins over amorphous Ni–P and Ni–B alloys, J. Chem. Soc. Faraday Trans. 180 (1984) 1435–1446.
[12] C.L. Fernando, G.Q. Santiago, A. Claudia, M.A. Keane, Gas phase hydrogenation of p-chloronitrobenzene over Pd–Ni/$Al_2O_3$, Appl. Catal. A: Gen. 473 (2014) 41–50.
[13] N.S. Babu, N. Lingaiah, P.S.S. Prasad, Characterization and reactivity of $Al_2O_3$ supported Pd–Ni bimetallic catalysts for hydrodechlorination of chlorobenzene, Appl. Catal. B: Environ. 111–112 (2012) 306–309.
[14] J. Zhao, L. Ma, X.L. Xu, F. Feng, X.N. Li, Synthesis of carbon-supported Pd/$SnO_2$ catalyst for highly selective hydrogenation of 2,4-difluoronitrobenzene, Chin. Chem. Lett. 25 (2014) 1137–1140.
[15] H. Yang, D. Shi, S.F. Ji, D.N. Zhang, X.F. Liu, Nanosized Pd assembled on superparamagnetic core–shell microspheres: synthesis, characterization and recyclable catalytic properties for the Heck reaction, Chin. Chem. Lett. 25 (2014) 1265–1270.
[16] S.J.S. Basha, P. Vijayan, C. Suresh, D. Santhanaraj, K. Shanthi, Effect of order of impregnation of Mo and Ni on the hydrodenitrogenation activity of NiO-$MoO_3$/AlMCM-41 catalyst, Ind. Eng. Chem. Res. 48 (2009) 2774–2780.
[17] A.B. Jaap, V. Tom, R.G.L. Bob, et al., Envisaging the physicochemical processes during the preparation of supported catalysts: Raman microscopy on the impregnation of Mo onto $Al_2O_3$ extrudates, J. Am. Chem. Soc. 126 (2004) 14548–14556.
[18] Y. Qiu, L. Xin, W.Z. Li, Electrocatalytic oxygen evolution over supported small amorphous Ni–Fe nanoparticles in alkaline electrolyte, Langmuir 30 (2014) 7893–7901.
[19] X.Q. Pan, Y.B. Zhang, Z.Z. Miao, X.G. Yang, A novel PdNi/$Al_2O_3$ catalyst prepared by galvanic deposition for low temperature methane combustion, J. Energy Chem. 22 (2013) 610–616.
[20] X.Q. Pan, Y.B. Zhang, B. Zhang, et al., Influence of electronic effect on methane catalytic combustion over PdNi/$Al_2O_3$, Chem. Res. Chin. Univ. 29 (2013) 952–955.
[21] P. Lu, T. Teranishi, K. Asakura, M. Miyake, N. Toshima, Polymer-protected Ni/Pd bimetallic nano-clusters: preparation, characterization and catalysis for hydrogenation of nitrobenzene, J. Phys. Chem. B 103 (1999) 9673–9682.
[22] P.K. Cheekatamarla, A.M. Lane, Efficient bimetallic catalysts for hydrogen generation from diesel fuel, Int. J. Hydrog. Energy 30 (2005) 1277–1285.
[23] D. Dissanayake, M.P. Rosynek, K.C.C. Kharas, J.H. Lunsford, Partial oxidation of methane to carbon monoxide and hydrogen over a nickel/alumina catalyst, J. Catal. 132 (1991) 117–127.



Please cite this article in press as: Y.-S. Feng, et al., Characterization and reactivity of $\gamma$-$Al_2O_3$ supported Pd–Ni bimetallic nanocatalysts for selective hydrogenation of cyclopentadiene, Chin. Chem. Lett. (2015), http://dx.doi.org/10.1016/j.cclet.2015.03.006